Application of signal-processing techniques to improve FDTD simulation results of resonant cavities

João Guilherme Dal Molin and Walter Pereira Carpes Jr.

Abstract—**This paper presents the application of two signal-processing techniques, *Hanning window* and *zero padding*, to the results of simulations of propagating waves using the FDTD method. Two problems involving rectangular resonant cavities are addressed: an empty cavity and a cavity partially filled with a dielectric. Frequency spectrum plots and tables with the numerical results demonstrate the difference between the results obtained from the simulations with and without the use of these techniques, highlighting the improvements in the graphs clarity and resolution as well as in the accuracy of the numerical results.**

Keywords— FDTD, cavity, microwaves, signal processing.

I. INTRODUCTION

Problems involving propagating microwave fields are becoming increasingly frequent and, hence, methods for solving these problems are constantly being explored. Analysis of electromagnetic fields in resonant cavities have an important role in the development and testing of new techniques that improve numerical calculation of propagating fields. Furthermore, resonant cavities are used for many applications in engineering, such as microwave transmitters and receivers, bandpass filters, microwave ovens, oscillators etc.

The finite-difference time-domain (FDTD) method is a powerful tool used to solve electromagnetic problems in the time domain. Problems involving field propagation in free space, antennas, diffractive optics, reverberation chambers and many other related subjects can be solved by this numerical technique, presented by Yee in 1966 [1]. This method, combined with the utilization of the *fast Fourier transform* (FFT) and other signal-processing techniques such as windowing and *zero padding*, can lead to very detailed analysis of the resonant cavities.

In computational simulations of resonant cavities, after the application of the FFT to the set of field samples, the resulting spectrum may have low frequency resolution, making it difficult to extract resonant frequency values with good accuracy. Aiming to gather information about the effect of the application of some signal-processing techniques in FFT graphs resolution and in the accuracy of numerical results, this paper presents the application of the *Hanning window* function and *zero padding* to two different problems involving rectangular resonant cavities – one consisting of an empty cavity and the other of a cavity partially filled with a dielectric material – both simulated by a computational program developed in MATLAB.

II. NUMERICAL ANALYSIS TECHNIQUE

The FDTD method is a numerical analysis technique used to solve Maxwell's curl equation by discretizing the time and space derivatives of the electric and magnetic fields.

João Guilherme Dal Molin, Departamento de Engenharia Elétrica e Eletrônica, Universidade Federal de Santa Catarina, Florianópolis - SC, e-mail: joaoguilhermedalmolin@gmail.com; Walter Pereira Carpes Jr., Departamento de Engenharia Elétrica e Eletrônica, Universidade Federal de Santa Catarina, Florianópolis - SC, e-mail: walterpcjr@gmail.com.

The Maxwell's curl equations can be written as following [2]:

$$\frac{\partial \vec{B}}{\partial t} = -\vec{\nabla} \times \vec{E} - \vec{J}_m \tag{1}$$

$$\frac{\partial \vec{D}}{\partial t} = \vec{\nabla} \times \vec{H} - \vec{J}_e \tag{2}$$

where $\vec{J}_m$ and $\vec{J}_e$ are the magnetic current density vector and the electric current density vector, respectively.

Considering the discretization of both time and space domains, the method usually uses a second-order accurate central-difference approximation to the derivatives:

$$f'(x) = \frac{f(x + \Delta x) - f(x - \Delta x)}{2\Delta x} + O((\Delta x)^2) \tag{3}$$

where the last term represents the remainder term (which is not included in the numerical solution), corresponding to the approximation error.

Further, the Maxwell's curl equations in the discrete domain form can be obtained by separating the electric and the magnetic field vector components and applying the central-difference derivative to (1) and (2). Assuming the use of cartesian coordinates, the example for the H_x equation is shown below:

$$\frac{H_x^{n+\frac{1}{2}}(i,j,k) - H_x^{n+\frac{1}{2}}(i,j,k)}{\Delta t} =$$
$$= \frac{1}{\mu_x(i,j,k)} \left(\frac{E_y^n(i,j,k+1) - E_y^n(i,j,k)}{\Delta z} \right.$$
$$- \frac{E_z^n(i,j,k+1) - E_z^n(i,j,k)}{\Delta y}$$
$$\left. - \sigma_{mx}(i,j,k)H_x^n(i,j,k) - J_{mix}^n(i,j,k) \right) \tag{4}$$

Here, the notation used is similar to the one presented in the 1966 Yee's paper [1] and Taflove's book [3], with slight differences. In this notation, i, j and k represent the indices of the elements of the matrices where the fields components values are stored in during the simulation (Fig. 1 and Fig. 2).

Fig. 1.   Notation of the indices of the elements of the matrices where the electric field components are stored in the computational program.

$$H_x\left(i(\Delta x-1),j\left(\Delta y-\frac{1}{2}\right),k\left(\Delta z-\frac{1}{2}\right)\right) \rightarrow H_x(i,j,k)$$

$$H_y\left(i\left(\Delta x-\frac{1}{2}\right),j(\Delta y-1),k\left(\Delta z-\frac{1}{2}\right)\right) \rightarrow H_y(i,j,k)$$

$$H_z\left(i\left(\Delta x-\frac{1}{2}\right),j\left(\Delta y-\frac{1}{2}\right),k(\Delta z-1)\right) \rightarrow H_z(i,j,k)$$

Fig. 2. Notation of the indices of the elements of the matrices where the magnetic field components are stored in the computational program.

The n and $n+\frac{1}{2}$ index indicate the sampling instants $n\Delta t$ and $\left(n+\frac{1}{2}\right)\Delta t$ in the time domain, respectively, where Δt is the step size. Fig. 3 illustrates the space discretization according to the Yee grid as well as a visualization of how a curl operation is calculated in it.
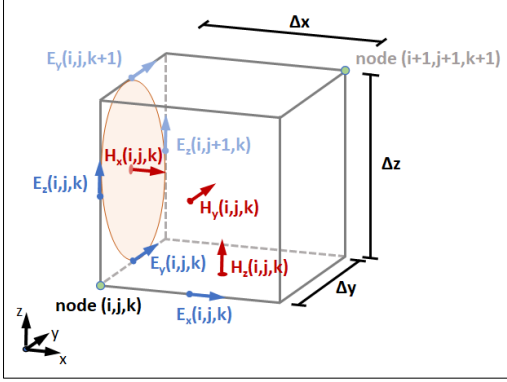

Fig. 3. Space discretization according to the Yee grid how a curl operation is calculated in it.

Fig. 4 shows how the instants are arranged in the discrete time domain, in what is called the *leapfrog scheme*:
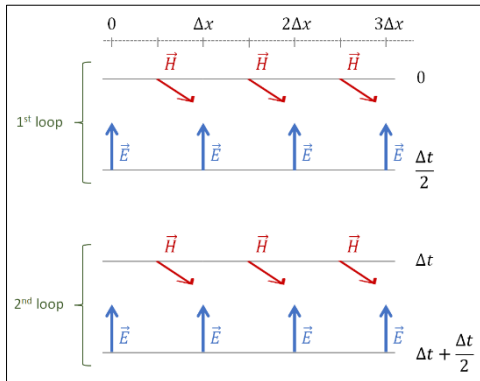

Fig. 4. Illustration of the *leapfrog scheme*, the staggering of the time instants in the time the domain.

Now, having these discretization concepts, the necessary equations and the proper notation in mind, it is easier to see that the equation (4) leads to an *FDTD update equation*:

$$\begin{aligned}H_x^{n+\frac{1}{2}}(i,j,k) = \ &C_{hxh}(i,j,k)H_x^{n-\frac{1}{2}}(i,j,k)\\ &+C_{hxey}(i,j,k)\left(E_y^n(i,j,k+1)\right.\\ &\left.-E_y^n(i,j,k)\right)\\ &+C_{hxez}(i,j,k)\left(E_z^n(i,j+1,k)\right.\\ &\left.-E_z^n(i,j,k)\right)\\ &+C_{hxjm}(i,j,k)J_{mix}^n(i,j,k)\end{aligned} \tag{5}$$

where:

$$C_{hxh}(i,j,k) = \frac{2\mu_x(i,j,k)-\Delta t\sigma_{mx}(i,j,k)}{2\mu_x(i,j,k)+\Delta t\sigma_{mx}(i,j,k)} \tag{6}$$

$$C_{hxey}(i,j,k)\frac{2\Delta t}{(2\mu_x(i,j,k)+\Delta t\sigma_{mx}(i,j,k))\Delta z} \tag{7}$$

$$C_{hxez}(i,j,k) = -\frac{2\Delta t}{(2\mu_x(i,j,k)+\Delta t\sigma_{mx}(i,j,k))\Delta y} \tag{8}$$

$$C_{hxjm}(i,j,k) = -\frac{2\Delta t}{2\mu_x(i,j,k)+\Delta t\sigma_{mx}(i,j,k)} \tag{9}$$

The method allows assigning different values of the properties of the medium where the fields exist at different positions, which allows the analysis of problems involving non-homogeneous materials.

III. NUMERICAL STABILITY AND SIZES OF CELLS

The values of Δt were calculated following the Courant-Friedrichs-Lewy stability condition, consulted from the Taflove's book from 1995 [3]:

$$\Delta t \leq \sqrt{\mu\varepsilon}\sqrt{\left(\frac{1}{\Delta x}\right)^2+\left(\frac{1}{\Delta y}\right)^2+\left(\frac{1}{\Delta z}\right)^2} \tag{10}$$

The sizes of the cells were chosen considering the geometry divisibility and the criterion also consulted from Taflove's work [3]:

$$\Delta x, \Delta y \text{ and } \Delta z \leq \frac{\lambda}{10} \tag{11}$$

As the simulation of the cavity partially filled with dieletric used magnetic properties to simulate symmetry, the sizes used for Δx and Δy had to minimize the imprecision caused by the staggered positions of the electric and the magnetic properties.

IV. PROBLEMS CONFIGURATIONS AND PARAMETERS

Two different configurations were used to verify the validity of using signal processing techniques to improve the results obtained with de FDTD method.

The first configuration consists of an empty cavity measuring 80 mm × 50 mm × 20 mm. The simulation of this problem uses cubic cells with 1 mm side and is executed twice – one with 2^{17} and other with 2^{15} time steps, both using $\Delta t = 1,11$ ms. The second example is a cavity partially filled with a dielectric material of $\varepsilon_r = 16$, as shown in Fig. 5. Actually, in this case, two magnetic walls were used to simulate symmetry and reduce the cavity in a quarter.
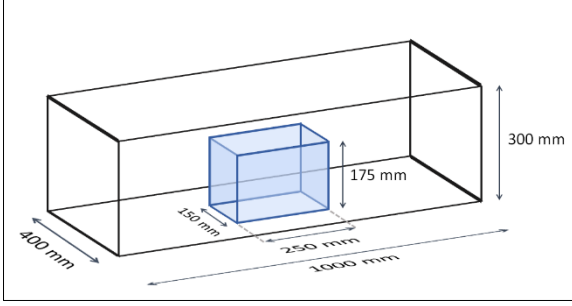
Fig. 5.   Configuration of the cavity partially filled with a dielectric.

The sizes of the cells used in this simulation are:

$$dx \cong 0.99750623441396508728179 55 \; mm$$

$$dy \cong 0.999000999000999000999 0010 \; mm$$

$$dz = 6{,}25 \; mm$$

and the number of time steps is 2^{18}, with $\Delta t = 2.1057$ ps.

V. SPECTRAL ANALYSIS

For each problem, the resonant frequencies were obtained by applying the *fast Fourier transform* (FFT) to a set of field samples at an arbitrary point of the space domain. This set of samples usually consists of the values of a field component in all the time steps of the simulation, though these sample values may also be taken only at certain time steps separated by a fixed interval. The numbers of time steps are powers of 2 due to the FFT implementation.

The spectral analysis of the empty cavity simulation was made for frequencies up to 600 MHz and its resonant frequencies were compared with the analytical results obtained using:

$$f_r = \frac{1}{2\sqrt{\mu\varepsilon}} \sqrt{\left(\frac{m}{a}\right)^2 + \left(\frac{n}{b}\right)^2 + \left(\frac{p}{c}\right)^2} \qquad (12)$$

where a, b, and c are the sizes of the resonant cavity in each cartesian dimension and m, n and p are natural numbers that indicate the propagation modes of the electromagnetic waves inside the cavity.

The analysis of the partially filled cavity included frequencies up to 10 GHz. The resonant frequencies obtained by the simulation were compared to the results obtained by Bardi *et al.* [4].

VI. SIGNAL-PROCESSING TECHNIQUES

Two signal processing techniques were applied to the numerical results to facilitate the visualization of resonance peaks, improve the accuracy of their resonance frequencies, enable certain analyses, or reduce the computer memory used to store the output data.

As the type of window used affects the spectrum plot obtained by the FFT, its choice is crucial for plot analysis. When the FFT is executed over only a time interval of the simulation (or the simulation just stops and the FFT is then applied to it), that means that a rectangular window is being used. This windowing is not always the best choice, as it may lead to a plot

that makes some resonant frequencies impossible to be observed.

The *Hanning window* [5], represented by the graph in Fig. 6, is applied by multiplying its amplitude at each sampling instant by the corresponding field samples.
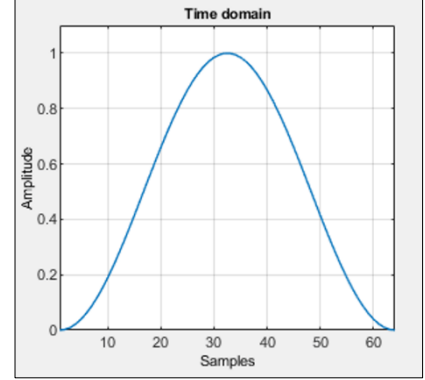

Fig. 6.   Graph representation of a Hanning window.

The other signal-processing technique tested in this simulation for comparison is the *zero padding* technique [5], which consists of adding zeros to the time series of field samples to increase the number of points in the FFT graph, improving the frequency resolution. In all the problems, the number of zeros added to the time series were 4 times the previous number of its elements, as shown in Fig. 7.
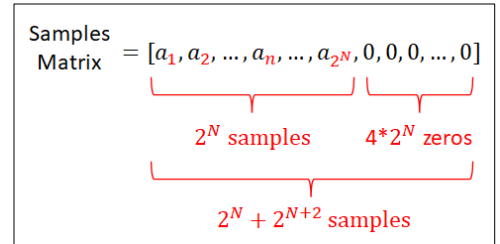

Fig. 7.   Zeros added to the samples array by the zero padding technique.

VII. RESULTS

The comparison between parts of the FFT graphs for the empty cavity simulation obtained without and with the Hanning window can be seen in Figs. 8 and 9, respectively.
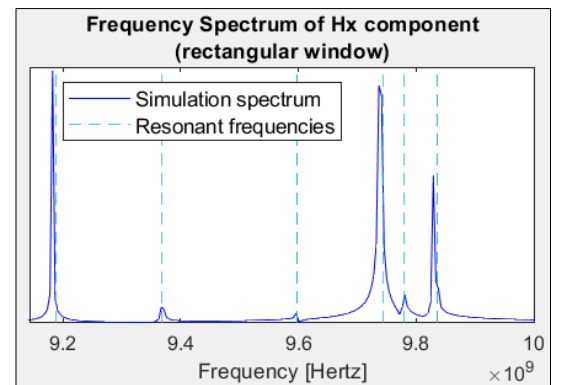

Fig. 8.   Frequency spectrum of the H_x component of the empty cavity simulation without using the Hanning window.
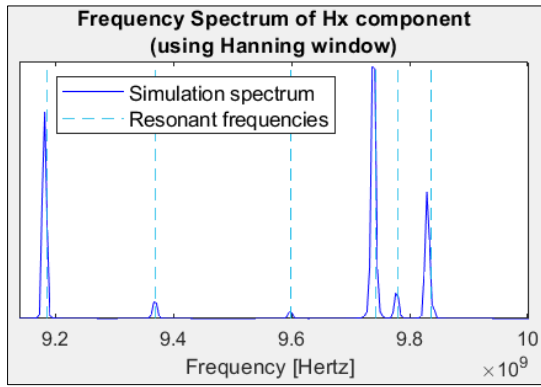
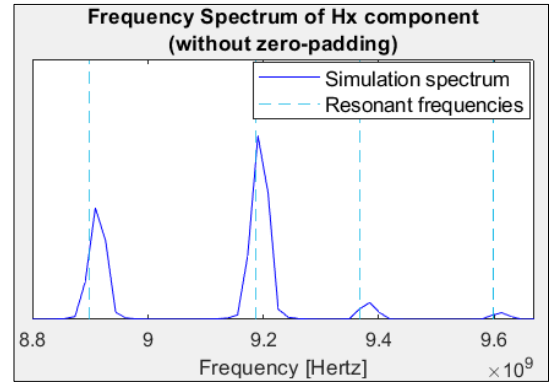Fig. 9.   Frequency spectrum of the H_x component of the empty cavity simulation using the Hanning window.

The FFT graphs, showing the frequencies from 350 to 550 MHz, resulted from the simulation of the cavity partially filled with a dielectric without and with the use of the Hanning window, respectively, are presented in Figs. 10 and 11.
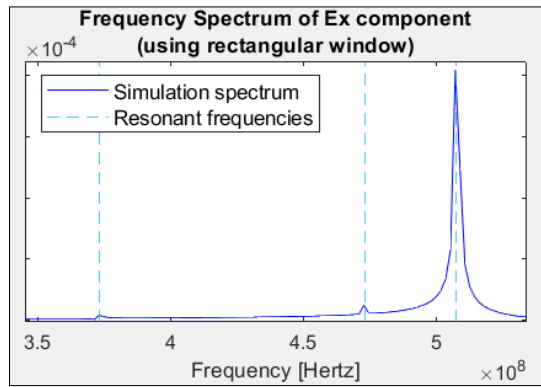

Fig. 10.   Frequency spectrum of the E_x component of the partially filled cavity simulation without using the Hanning window.
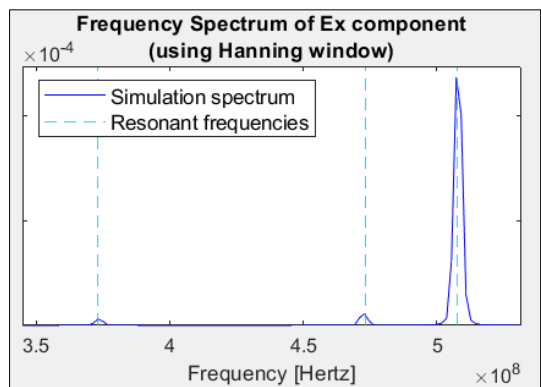

Fig. 11.   Frequency spectrum of the E_x component of the partially filled cavity simulation using the Hanning window.

The frequency spectrum graph, from 8.8 GHz to 9.67 GHz, of the simulation of the empty cavity problem executed with 2^{15} time steps, without and with the utilization of zero padding, are shown, respectively, in Figs. 12 and 13.

Fig. 12.   Frequency spectrum of the H_x component of the empty cavity simulation without the use of zero padding.
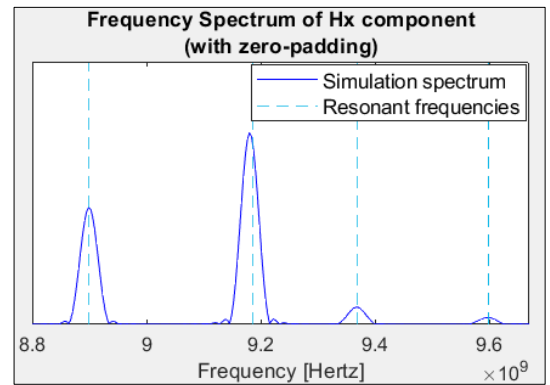

Fig. 13.   Frequency spectrum of the H_x component of the empty cavity simulation with the use of zero padding.

Table I presents a comparison between the analytical values of the resonant frequencies and their corresponding peak values of the frequency spectrum obtained by the simulations of the empty cavity executed with 2^{15} time steps, with and without the use of signal-processing techniques.

TABLE I.   COMPARISON BETWEEN RESONANT FREQUENCIES OF THE EMPTY CAVITY SIMULATED FOR 2^{15} TIME STEPS WITH DIFFERENT COMBINATIONS OF SIGNAL-PROCESSING TECHNIQUES.

Analytical	Rectangular window and no zero padding		Hanning window		Hanning window and zero padding	
value (GHz)	value (GHz)	error (%)	value (GHz)	error (%)	value (GHz)	error (%)
3.535	3.557	0.62	3.557	0.62	3.539	0.11
4.799	4.824	0.52	4.824	0.52	4.803	0.08
6.282	6.303	0.33	6.303	0.33	6.282	0.00
6.371	6.391	0.31	6.391	0.31	6.374	0.05
7.071	7.078	0.10	7.078	0.10	7.071	0.00
7.726	7.730	0.05	7.730	0.05	7.722	0.05
8.072	8.082	0.12	8.082	0.12	8.071	0.01
8.219	8.240	0.26	8.240	0.26	8.219	0.00
8.287	8.311	0.29	8.293	0.07	8.286	0.01

8.380	8.399	0.23	8.399	0.23	8.377	0.04
8.900	8.909	0.10	8.909	0.10	8.899	0.01
9.187	9.191	0.04	9.191	0.04	9.180	0.08
9.369	9.385	0.17	9.385	0.17	9.367	0.02
9.598	9.596	0.02	9.614	0.17	9.599	0.01
9.743	9.754	0.11	9.754	0.11	9.737	0.06
9.779	9.790	0.11	-	-	9.786	0.07
9.837	9.842	0.05	9.842	0.05	9.828	0.09

The resonant frequencies obtained from the previous problem, with and without the use of the same signal-processing techniques, but this time simulated with 2^{17} time steps, are given in Table II, along with the values obtained analytically.

TABLE II. COMPARISON BETWEEN RESONANT FREQUENCIES OF THE EMPTY CAVITY SIMULATED FOR 2^{17} TIME STEPS WITH DIFFERENT COMBINATIONS OF SIGNAL-PROCESSING TECHNIQUES.

Analytical	Rectangular window and no zero padding		Hanning window		Hanning window and zero padding	
value (GHz)	value (GHz)	error (%)	value (GHz)	error (%)	value (GHz)	error (%)
3.535	3.539	0.10	3.539	0.10	3.536	0.03
4.799	4.802	0.07	4.802	0.07	4.799	0.00
6.282	6.281	0.01	6.281	0.01	6.280	0.03
6.371	6.374	0.05	6.374	0.05	6.369	0.03
7.071	7.074	0.04	7.074	0.04	7.068	0.04
7.726	7.725	0.01	7.725	0.01	7.720	0.08
8.072	8.073	0.01	8.073	0.01	8.068	0.05
8.219	8.223	0.05	8.223	0.05	8.217	0.02
8.287	8.289	0.02	8.289	0.02	8.283	0.05
8.380	8.377	0.03	8.377	0.03	8.375	0.06
8.900	8.900	0.01	8.900	0.01	8.897	0.03
9.187	9.182	0.05	9.182	0.05	9.178	0.10
9.369	9.367	0.02	9.367	0.02	9.365	0.04
9.598	9.596	0.02	9.596	0.02	9.594	0.04
9.743	9.737	0.07	9.737	0.07	9.735	0.08
9.779	9.781	0,02	9.780	0.02	9.775	0.04
9.837	9.829	0,08	9.838	0.02	9.827	0.10

Table III presents a comparison between the analytical values of the resonant frequencies and their corresponding peak values of the frequency spectrum obtained in the simulations of the partially filled cavity executed with 2^{18} time steps, with and without the use of signal-processing techniques.

TABLE III. COMPARISON BETWEEN RESONANT FREQUENCIES OF THE PARTIALLY FILLED CAVITY SIMULATED WITH DIFFERENT COMBINATIONS OF SIGNAL-PROCESSING TECHNIQUES.

Analytical	Rectangular window and no zero padding		Hanning window		Hanning window and zero padding	
value (MHz)	value (MHz)	error (%)	value (MHz)	error (%)	value (MHz)	error (%)
256.7	259.1	0.93	259.1	0.93	258.0	0,51
373.0	373.2	0.05	373.2	0.05	372.1	0,24
473.3	472.8	0.11	472.8	0.11	471.0	0,49
507.6	507.3	0.06	507.3	0.06	506.5	0,22
553.7	554.4	0.13	554.4	0.13	552.2	0,27
592.3	590.6	0.29	590.6	0.29	592.0	0,05

VIII. CONCLUSION

By the comparisons between Figs. 8 and 9 and between Figs. 8 and 9, it is visible that the application of the Hanning window to the array of field samples highlights the resonant frequencies in the FFT graph. The first and the second peaks are almost undetected in Fig. 10, which shows the FFT graph of the partially filled cavity simulation with the use of rectangular window. However, according to Table I, Table II and Table III, the Hanning window by itself made negligible or no difference in the values obtained in the simulations, with few exceptions.

Zero padding, in its turn, improved the results for the empty cavity simulation with low sample rate (Table I), even making two resonant frequencies visible. On the other hand, it didn't contribute significantly to the simulation with a higher sample rate (Table II) and, in addition, it increased the error of the values obtained from the partially filled cavity simulation (Table III), which also has a relatively high sample rate. Figs. 11 and 10 highlight the differences in resolution and in accuracy of the FFT graph from the empty cavity simulation with 2^{15} time steps.

Thus, the use of Hanning window was relevant to improve the resolution and clarity of the spectrum graphs, while it did not make significant difference on the accuracy of resonant frequencies values. As the aim of the zero padding technique consists of increasing the spectrum frequency resolution, its utilization was only pertinent for simulations with a sample rate lower than a certain number, which depends on the geometry and parameters of each problem.

REFERENCES

[1] K. S. Yee, "Numerical Solution of Initial Boundary Value Problems Involving Maxwell's Equations in Isotropic Media", *IEEE Transitions on Antennas and Propagation*, v. ap-14, no. 3, pp. 302–307, May 1966.

[2] A. Elsherbeni and V. Demir, *The Finite-Difference Time-Domain Method for Electromagnetics with MATLAB® Simulations.* 1. ed. SciTech Publishing, 2009.

[3] A. Taflove, *Computation Electrodynamics: The Finite-Difference Time-Domain Method*. 1. ed. Artech House, 1995.

[4] I. Bardi, O. Biro and K. Preis, "Finite element scheme for 3D cavities without spurious modes", *IEEE Transactions on Magnetics*, vol. 27, no. 5, pp. 4036-4039, Sept 1991.

[5] J. O. Smith, *Spectral Audio Signal Processing*. W3L Publishing, 2011.